Quantum Fluctuations due to Spinons, Polarons, and Stripes in the Two-Dimensional Hubbard Model

Norikazu Tomita and Shuji Watanabe
Yamagata University, 1-4-12 Kojirakawa, Yamagata, 990-8560, Japan
(Received 28 January 2009; published 9 September 2009)

Quantum fluctuations (QF's) in the two-dimensional Hubbard model are visualized by superposition of optimized nonorthogonal Slater determinants. In the half-filled system, QF's consist of rotational and translational motions of spinon-antispinon pairs, while in the lightly doped systems ($\delta = 0.96$), those motions of polarons form the QF's. It is shown that an attractive interaction works between two polarons, in the framework of a projected Hartree-Fock picture. At about 10% doping, the ground state has a stripe structure and QF's due to deviations from the uniform stripe. The present method gives the ground state energies comparable or in some cases superior to the variational Monte Carlo method with a Gutzwiller projection parameter.

DOI: 10.1103/PhysRevLett.103.116401 PACS numbers: 71.10.Fd, 71.15.−m

Large quantum fluctuations (QF's) in interacting fermion systems have been one of the central issues in not only condensed-matter but also particle physics. Especially, since the discovery of high-temperature superconductors, the two-dimensional (2D) electron system has been a challenging target for theorists to try their many-body methodologies. Numerical approaches, such as a quantum Monte Carlo (QMC) simulation [1], a density matrix renormalization group [2], and a variational Monte Carlo (VMC) method [3], have been applied to copper oxides, and succeeded to explain some of their important properties in the framework of a 2D Hubbard model, such as an antiferromagnetism in the half-filled system and an insulator-metal transition by doping [4]. However, in these numerical approaches, we obtain information only through correlation functions or spectral functions. We cannot usually see how such many-body structures are realized or what units feel an attractive interaction. On the other hand, conceptional approaches, such as a spin bag [5], a resonating valence bond [6], and a FLEX [7] pictures, are direct and easy to understand what is going on in that system. But, it is difficult to estimate the accuracy of such conceptional pictures, because of the large correlation effects. In this Letter, we demonstrate that the electron correlation effects are reasonably described as QF's due to spinons, polarons, and stripes, by using a resonating Hartree-Fock (Res-HF) method. We will also show that an attractive interaction works between two polarons.

In the Res-HF method, a many-fermion wave function is constructed by superposition of nonorthogonal Slater determinants (S dets) [8], such as

$$|\Psi\rangle = \sum_{n=1}^{N_S} C_n \sum_G P^G |\phi_n\rangle. \quad (1)$$

Here, N_S denotes the number of S dets. The molecular orbitals of all the S dets $|\phi_n\rangle$, as well as their coefficients C_n, are simultaneously optimized to minimize the Res-HF energy. Nonorthogonality of S dets allows us to describe the correlation effects efficiently [9,10]. In this method, the DODS-type S dets are employed to incorporate the correlation effects from symmetry broken states. To recover the symmetry of the system, we adopt symmetry projections (SP's) for each S det, which are symbolically denoted by P^G in Eq. (1). In the following, we consider a square lattice with a periodic boundary condition, which has a D_4 and translation symmetries. The SP corresponds to superposition of the Goldstone set for each symmetry broken state. Details of the SP are given in Ref. [11]. Unique and important feature of the present method is that we can visualize QF's by analyzing the structures of S dets. This is the essential difference from other numerical approaches. For example, a large nuclear deformation in the transition region of even nuclei was reasonably described by superposition of prolate and oblate shapes [12]. In this Letter, we apply the Res-HF method for the 2D Hubbard models.

The 2D Hubbard model is a standard model for interacting electrons in layered materials, such as copper-oxides. Its Hamiltonian is given by

$$H = -t \sum_{\langle i,j\rangle\sigma}^{N} (a_{i,\sigma}^{\dagger} a_{j,\sigma} + a_{j,\sigma}^{\dagger} a_{i,\sigma}) + U \sum_{i}^{N} n_{i,\uparrow} n_{i,\downarrow}, \quad (2)$$

where t, U, and N represent a nearest-neighbor hopping, an on-site Coulomb repulsion and a system size, respectively. In the following, we focus on the normal states which conserve a global gauge symmetry. The number of electrons is denoted by N_e, and the energies are scaled by t.

First, we mention the Res-HF ground state energies. For a small cluster of $N = 4 \times 4$, the Res-HF wave functions with 5 S dets well reproduce the exact diagonalization calculations [13,14]. For example, in the case of $U/t = 8$, the Res-HF energies are -8.46 for the half-filled system ($E_{\text{exact}} = -8.47$) and -11.81 for $N_e = 14$ ($E_{\text{exact}} = -11.87$). Then, we compare the ground state energies for

much larger systems ($N = 8 \times 8$). In the case of a half-filled system, the Res-HF wave function with $N_S = 10$ S dets gives the total energy of -32.8 for $U/t = 8$, while the VMC wave function with a Gutzwiller (GW) projection parameter (PP) gives -31.6 [15]. On the other hand, a new VMC wave function, which includes an additional PP promoting hole motion and kinetic exchange to a GW one, gives -32.9 [16]. In the weaker interaction regime, for example, at $U/t = 4$, a Gaussian basis Monte Carlo method was applied and its energy was -55.0 [17], while the Res-HF method($N_S = 10$) gives -54.7. In the case of a doped system with $N_e = 60$, the Res-HF wave function with $N_S = 10$ S dets gives the total energy of -32.5 for $U/t = 10$. The VMC wave function with a GW PP on an antiferromagnetic reference gives -32.1, while the VMC wave function with a HF-Bogoliubov(HFB)-type reference gives -33.3 [18]. The BCS-type reference significantly lowers the VMC energy for the doped system. In this Letter, however, we focus on the QF's in the normal states, since they would give a clue to understand the mechanism of the high-T_C superconductivity. The orbital optimization makes the Res-HF wave functions converge in the same quality even if we start with different trial S dets. Thus, the Res-HF method provides reliable wave functions.

In the present research, the parameters (t, U) are set at (1.0, 8.0), which would be reasonable for the copper-oxides since some experimental data are explained with these values [19]. In most cases, the system size is $N = 10 \times 10$, and $N_S = 10$ S dets are employed to generate the Res-HF wave functions. The correlation energies explained by the Res-HF method are increased with the increase of N_S. For example, at $U/t = 8$, the wave functions with $N_S = 2$, 5, and 10 S-dets give the ground state energies of -49.9 (-54.1), -50.2 (-54.5), and -50.4 (-54.7), respectively, for the half-filled ($N_e = 96$) system. Although the further increase of N_S will lower the energies, physics for QF's, shown below, is not largely affected. 10 S dets are enough to obtain substantial information on QF's.

Figure 1 shows the structures of three typical S dets generating the Res-HF wave function at a half-filling. Here, ASD (or NSD) is short for the alternating (or net) component of the spin density (SD), and is given by

$$\mathrm{SD}\,(l_x, l_y) \equiv \langle a^\dagger_{(l_x,l_y)\uparrow} a_{(l_x,l_y)\uparrow} - a^\dagger_{(l_x,l_y)\downarrow} a_{(l_x,l_y)\downarrow} \rangle = \mathrm{NSD}(l_x, l_y) + (-1)^{(l_x+l_y-1)} \mathrm{ASD}(l_x, l_y). \quad (3)$$

The SD is shown in (a), where a blue (red) circle represents a site with up (down) SD. The size of a circle represents the amplitude of the SD. The ASD, depicted in (b), indicates the phase and amplitude of the SD wave (SDW). The NSD is shown in (c). We omit the figures showing the charge density (CD), since there is no significant charge modulation. Instead, the S dets have defects in the SDW which suppress the ASD and have NSD. The substantial structures are indicated by "T-shaped enclosures" in (a) and (c). There exists mismatch of the SDW in each enclosure.

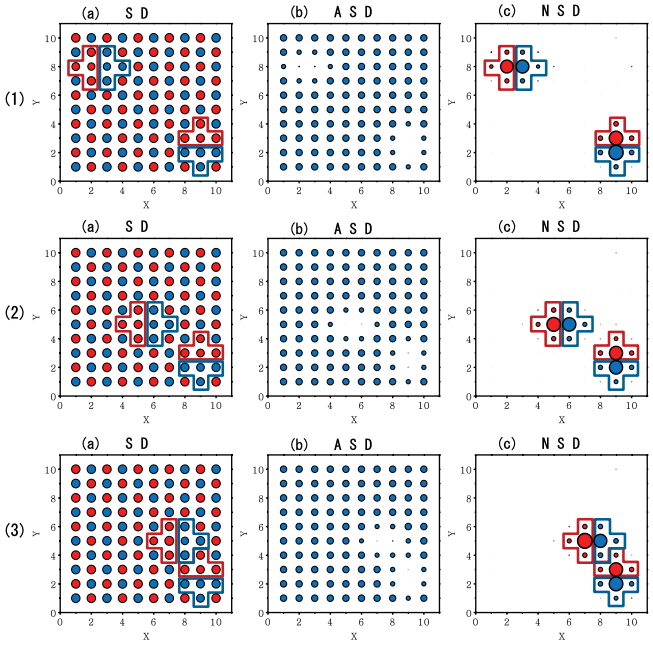

FIG. 1 (color). Structures of three typical S dets generating the Res-HF wave function for $N = N_e = 100$. SD and ASD are commonly scaled and their maximum value is 0.920. The maximum value of NSD is 0.677. The total energy is -50.4.

These defects are called spinons. Their property is similar to that of a neutral soliton in the 1D systems [20,21]. In contrast to the 1D system, spinon and antispinon ($S - \bar{S}$) are confined in the 2D system because their separation creates further mismatches of the SDW perpendicular to the pair direction. Figures 1(1) to 1(3) show two $S - \bar{S}$ pairs on different sites. Other S dets, which are not depicted here, also have $S - \bar{S}$ pairs. These S dets indicate vibration of $S - \bar{S}$ pairs (not inner motion of a single pair). As we superpose the Goldstone set of each S det, the QF's in the half-filled system are described by the translational and rotational motions of $S - \bar{S}$ pairs, as well as their vibrational motions.

Then, in Fig. 2, we show three typical S dets generating the Res-HF wave function for $N_e = 96$. The CD and its net (NCD) and alternating (ACD) components are given by

$$\mathrm{CD}\,(l_x, l_y) \equiv \langle a^\dagger_{(l_x,l_y)\uparrow} a_{(l_x,l_y)\uparrow} + a^\dagger_{(l_x,l_y)\downarrow} a_{(l_x,l_y)\downarrow} \rangle = \mathrm{NCD}(l_x, l_y) + (-1)^{(l_x+l_y-1)} \mathrm{ACD}(l_x, l_y). \quad (4)$$

Here, the NCD represents a hole density. Each S det has defects in the SDW, whose substantial structures are denoted by "cross-shaped enclosures" in (a). These defects suppress the ASD and induce the ACD as shown in (b) and (e). There exist both the NSD and NCD in these suppressed SDW regions, as seen from (c) and (f). We call these defects polarons, since they have similar properties to a polaron in the 1D system [21]. We should note that they can also be regarded as spin bags [5]. Figures 2(1) and 2(2) show four polarons on different relative positions. The S det shown in Fig. 2(3) has a $S - \bar{S}$ pair, as well as four

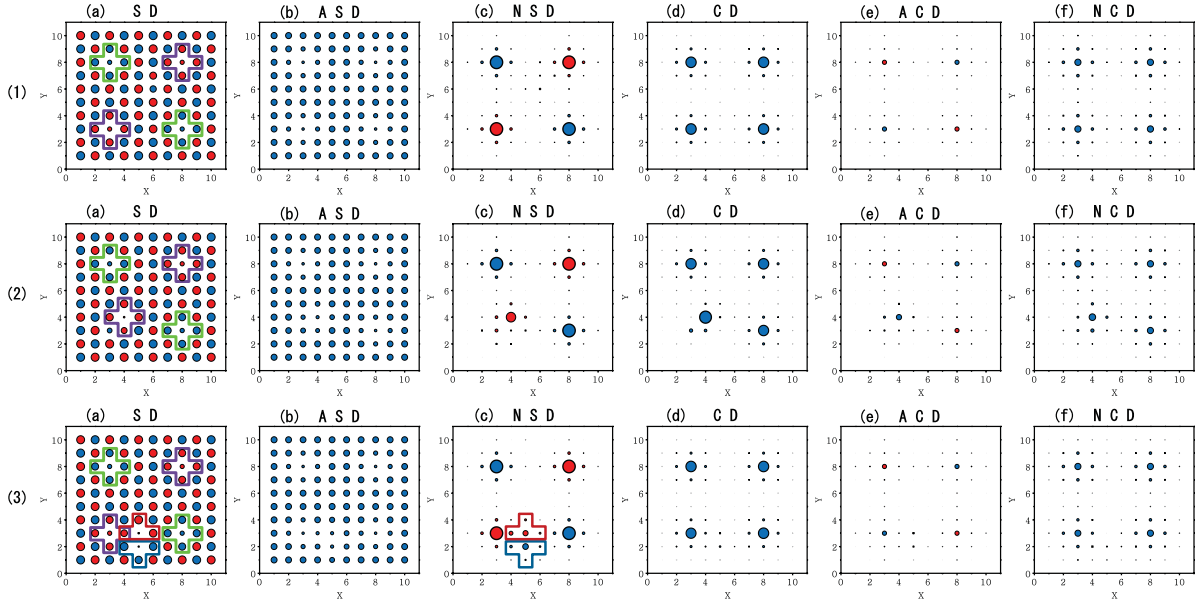

FIG. 2 (color). Structures of three typical S dets generating the Res-HF wave function for $N = 100$ and $N_e = 96$. Scales of SD, ASD, and NSD are the same as in Fig. 1. The maximum value of the SD and ASD in this figure is 0.906 while that of NSD is 0.626. CD, ACD and NCD are commonly scaled, and their maximum value is 0.524. The total energy is -54.7.

polarons. Other S dets, which are not depicted here, contain these polarons. Thus, the dominant QF's in the lightly doped system are described by translation and rotation of polarons as well as their vibration.

Here, let us consider how the energy of a polaron pair depends on distance. One of the remaining questions on the high-T_C superconductivity is what units feel an attractive interaction. In the unrestricted HF (UHF) approximation, the state having two polarons is a stable solution for $N_e = N - 2$ systems. As shown in Fig. 3, however, the UHF energies are getting higher as the distance of two polarons becomes closer. This means that an interaction between two polarons is repulsive in the UHF picture. To incorporate more correlation effects, we superpose the Goldstone set of the UHF solution. This is called a projected HF (pHF) approximation. As shown in Fig. 3, the pHF energies become lower as two polarons get closer. A size-dependence indicates that the result holds in the thermodynamic limit. This result suggests that an attractive interaction works between two polarons when we incorporate the electron correlation effects. To treat the superconducting state consistently with the normal state, we need a resonating HFB method [22]. Precise description on the superconducting state will be done in the near future.

Next, we show the structures of two typical S dets for $N_e = 92$ in Fig. 4. S det in Fig. 4(1) shows a clear stripe, while that in Fig. 4(2) has deviation from the uniform stripe. We have obtained these fluctuating stripe structures for $N_e = 92$ to $N_e = 88$. In Fig. 4(i), we show a typical S det for $N = 16 \times 16$ and $N_e = 224$ (12.5% doping). We can see the fluctuating stripe structures also in this larger system. The stripe structure was first pointed out by Tranquada *et al.* [23], and studied by many authors [24,25]. The present result is consistent with these previous works. For example, as seen from Fig. 4(i)(b), the phase of the SDW converts at the stripe. On the other hand, the Res-HF wave functions do not show a static stripe, but they show QF's due to deviations from the uniform stripe. These fluctuations would correspond to the dynamical stripe structures. A static stripe would be stabilized by other extra factors, such as an impurity [26] or electron-phonon coupling.

In summary, we have visualized a variety of the QF's in the 2D Hubbard model. In the half-filled system, QF's due to $S - \bar{S}$ pairs are dominant, while QF's due to polarons become dominant in the lightly doped system. The interaction between two polarons becomes attractive. This attractive interaction comes from the electron correlation

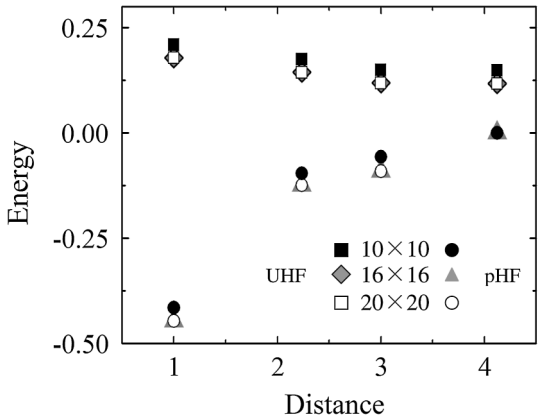

FIG. 3. Distance (d) dependence of energies of two-polaron states for $N_e = N - 2$ ($N = 100$, 256, and 400). The energies are measured from the pHF states at $d = \sqrt{17}$.

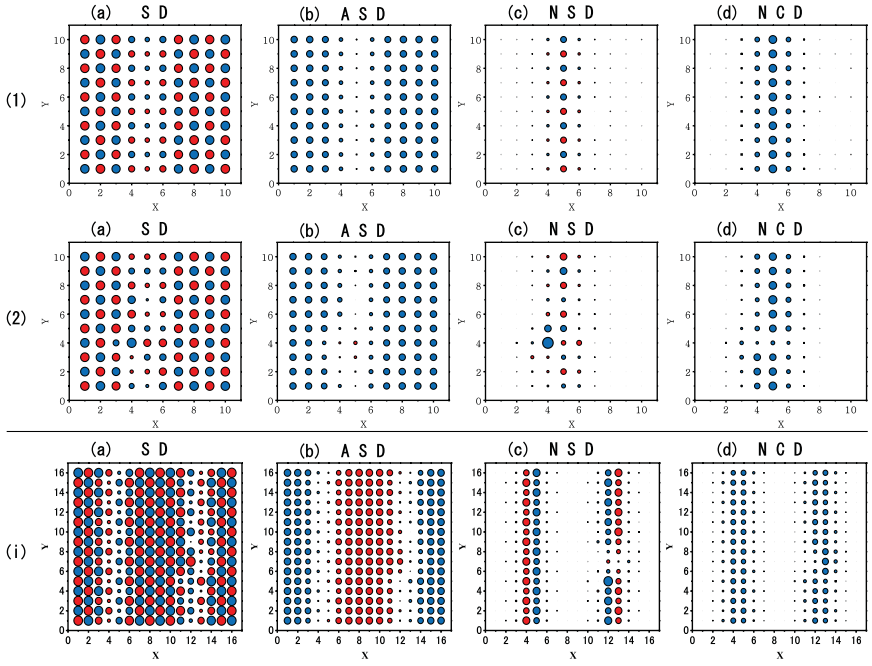

FIG. 4 (color). Structures of two typical S dets generating the Res-HF wave function for $N = 100$ and $N_e = 92$ [(1) and (2)]. The total energy is -59.6. A S det for $N = 16 \times 16$ and $N_e = 224$ is shown in (i). Both the NSD and NCD are induced along the vertical line where the ASD is suppressed. To save space, we omit the CD and ACD. The ACD component is small. Scale of each component is the same as in Fig. 2. The maximum value of SD and ASD is 0.936 while that of NSD is 0.490. The maximum value of NCD is 0.412.

effects, or resonance of the Goldstone set for the two-polaron state. Then, the stripe structure appears at about 10% hole doping with the QF's due to deviation from the uniform stripe. Although some extra factors, such as an electron-phonon interaction [27] or an interplane coupling [28], might be necessary to understand the copper-oxides precisely, the present direct description of the QF's would give a new light on the strongly correlated electron systems and high-T_C superconductivity.

The authors are grateful to Dr. A. Ikawa and Dr. M. Ozaki for fruitful discussion. This work was supported by the Next Super Computing Project, Nanoscience Program, MEXT, Japan.

[1] *Quantum Monte Carlo Method in Condensed Matter Physics*, edited by M. Suzuki (World Scientific, Singapore, 1993).
[2] S. R. White, Phys. Rev. Lett. **69**, 2863 (1992).
[3] H. Yokoyama and H. Shiba, J. Phys. Soc. Jpn. **56**, 3582 (1987).
[4] D. J. Scalapino, J. Supercond. Novel Magnetism **19**, 195 (2007).
[5] J. R. Schrieffer, X. G. Wen, and S. -C Zhang, Phys. Rev. Lett. **60**, 944 (1988).
[6] P. W. Anderson Science **235**, 1196 (1987).
[7] T. Moriya, Y. Takahashi, and K. Ueda, J. Phys. Soc. Jpn. **59**, 2905 (1990).
[8] H. Fukutome, Prog. Theor. Phys. **80**, 417 (1988).
[9] H. Koch and E. Dalgaard, Chem. Phys. Lett. **212**, 193 (1993).
[10] N. Tomita, S. Ten-no, and Y. Tanimura, Chem. Phys. Lett. **263**, 687 (1996).
[11] N. Tomita, Phys. Rev. B **69**, 045110 (2004).
[12] S. Nishiyama and H. Fukutome, J. Phys. G **18**, 317 (1992).
[13] E. Dagotto, A. Moreo, F. Ortolani, D. Poilblanc, and J. Riera, Phys. Rev. B **45**, 10 741 (1992).
[14] T. Tohyama, Y. Inoue, K. Tsutsui, and S. Maekawa, Phys. Rev. B **72**, 045113 (2005).
[15] H. Yokoyama, M. Ogata, and Y. Tanaka, J. Phys. Soc. Jpn. **75**, 114706 (2006).
[16] D. Eichenberger and D. Baeriswyl, Phys. Rev. B **76**, 180504(R) (2007).
[17] T. Aimi and M. Imada, J. Phys. Soc. Jpn. **76**, 113708 (2007).
[18] T. Giamarchi and C. Lhuillier, Phys. Rev. B **43**, 12 943 (1991).
[19] D. Eichenberger and D. Baeriswyl, Physica (Amsterdam) **460–462C**, 1153 (2007).
[20] W. P. Su, J. R. Schrieffer, and A. J. Heeger, Phys. Rev. Lett. **42**, 1698 (1979).
[21] H. Fukutome, J. Mol. Struct. (Theochem) **188**, 337 (1989).
[22] S. Nishiyama and H. Fukutome, Prog. Theor. Phys. **85**, 1211 (1991).
[23] J. M. Tranquada, B. J. Sternlieb, J. D. Axe, Y. Nakamura, and S. Uchida, Nature (London) **375**, 561 (1995).
[24] V. J. Emerly, S. A. Kivelson, and J. M. Tranquada, Proc. Natl. Acad. Sci. U.S.A. **96**, 8814 (1999).
[25] N. B. Christensen, H. M. Rϕnnow, J. Mesot, R. A. Ewings, N. Momono, M. Oda, M. Ido, M. Enderle, D. F. McMorrow, and A. T. Boothroyd, Phys. Rev. Lett. **98**, 197003 (2007).
[26] T. Tohyama, M. Takahashi, and S. Maekawa, Physica (Amsterdam) **357–360C**, 93 (2001).
[27] G.-H. Gweon, T. Sasagawa, S. Y. Zhou, J. Graf, H. Takagi, D.-H. Lee, and A. Lanzara, Nature (London) **430**, 187 (2004).
[28] H. Mukuda, M. Abe, Y. Araki, Y. Kitaoka, K. Tokiwa, T. Watanabe, A. Iyo, H. Kito, and Y. Tanaka, Phys. Rev. Lett. **96**, 087001 (2006).